Paper 77

©Civil-Comp Press, 2012
Proceedings of the Eighth International Conference
on Engineering Computational Technology,
B.H.V. Topping, (Editor),
Civil-Comp Press, Stirlingshire, Scotland

Modelling and Simulation Tests of an Electrohydraulic Servo-Drive with a Stepping Motor

A. Myszkowski
Institute of Mechanical Technology
Poznan University of Technology, Poland

Abstract

Linear electro hydraulic servo-drives have been built and used in various industrial equipment for more than sixty years. They are distinguished by the ability to develope extremely large forces with the positioning accuracy of the order of a micrometer, ensuring, at the same time, very good dynamic features.

The drives characterised by very slow motion and large force are used, among others, in presses, rolling mills, large machine tools, in mobile devices, such as building machinery, and in antennas and space telescopes where the observed objects require high accuracy [3, 5, 6]. These features are confirmed by many literature references cited in the present paper.

In order to ensure precise the control of electro hydraulic drives very expensive servovalves provided with torque motors or proportional valves are used [1, 2, 7, 8, 9, 10, 11]. The operational characteristics of the stepping motors indicate that they are able to make very small angular motions (steps) with high frequencies. This enables them to be used in driving elements that control very small fluxes [4, 5].

The present paper presents and discusses the construction of the hydraulic valve controlled with a stepping motor, construction of the whole servo-unit, and a complete stand for verification tests provided with a servo-drive. A mathematical description is presented of a four-edge hydraulic amplifier controlled by the stepping motor and a hydraulic servo-motor. Their models have been built and simulation tests have been carried out with the help of the Matlab-Simulink software. The phenomena characteristics for slow fluxes and small motion velocity are considered in the model. The test results are compared with the results of experimental tests and indicate good agreement and as a consequence the correctness of the simulation research.

The simulation tests and experimental verification of the electro hydraulic servo-drive with stepping motor confirm the use of the stepping motor to obtain a very small and accurate travel slide, thus ensuring the high accuracy of setting of the flux control valve. The servo-unit provided with such a valve may move with the speed of the order of 2μm/s.

Keywords: electrohydraulic servo-drive, low motion velocity, stepping motor,

1 Introduction

Formulation of basic theoretical relationships that describe the electro hydraulic servo-unit with stepping motor enable designing such a device and constructing its complex model that may be helpful for developing its computer model.

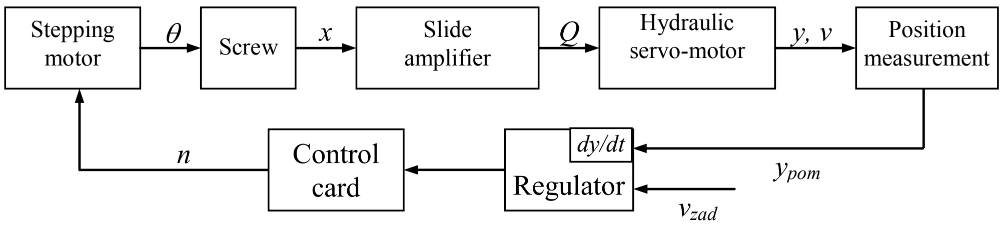

Figure 1: Block diagram of the electro hydraulic servo-drive provided with stepping motor and electric feedback.

Figure 1 presents a block diagram of the electro hydraulic servo-drive provided with stepping motor and electric feedback, being the object of consideration of the present paper. It consist of a stepping motor with a control card, slide amplifier, hydraulic servo-motor, position measuring system and the controller. The control valve with stepping motor shown in Fig. 2 is an independent electro-hydraulic device. It is so designed as to enable free assembling, without any mechanical modification, to servo-drives (servo-motors) available to the author of the present paper, instead of a servo-valve or proportional valve.
Required travel of the distribution valve slide is ensured by the stepping motor (1). The slide of the four-edge amplifier (3) is coupled to the motor shaft with a bellows clutch (2) and assembled to the valve body (5) with the bolt (6). The impulse transmitted to the control card results in such adjustment of the motor winding that its rotor makes one step rotation. In consequence, the slide is displaced into or out the valve body, in proportion to the screw pitch. This results in partial covering or uncovering of the slots of the sleeve (4) by the four-edge slide.

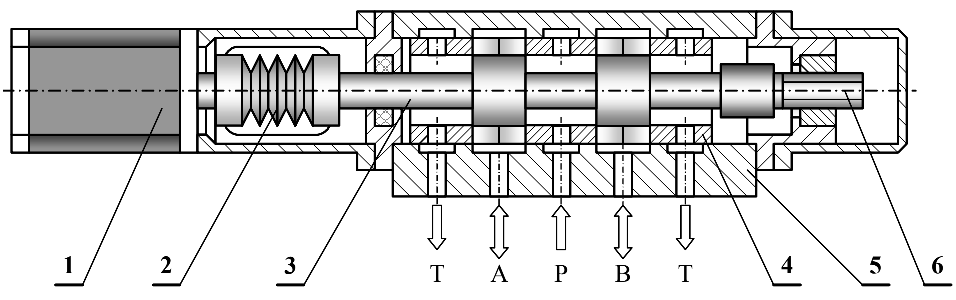

Figure 2: Control valve of the stepping motor.

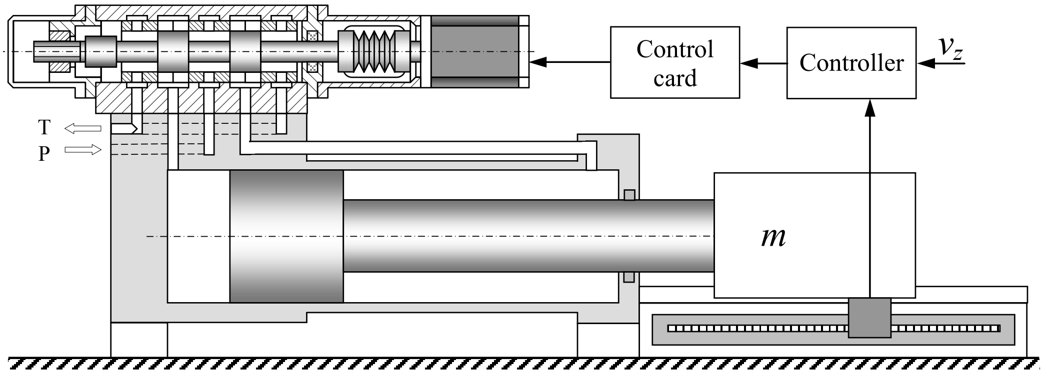

Figure 3: The electro hydraulic servo-drive with the stepping motor and electric feedback.

The servo-drive (Fig. 3) is provided with incremental optical system for measuring the position with 0.5μm resolution. Its slide is fixed directly to the part that is displaced by the piston rod. This ensures proper information on actual position at the drive outlet. The measuring system transmits the impulses that correspond to the position changes. Based on it the control system determines instantaneous speed of the servo-drive motion. Its value is subtracted from the set speed, while the difference is the control error that is then delivered to the controller. It generates a control signal transmitted to the motor control card, that distributes the power among particular windings of the stepping motor stator. The changes in the rotor positions result in opening and closing the working slots of the hydraulic amplifier and, in consequence, the changes in resistance of the liquid flowing to and from the chambers of the hydraulic servo-motor.

2 Model of the setting assembly with the stepping motor and its control system

Block diagram of the element setting the slide of the electro hydraulic amplifier is shown in Fig. 4a. The simulation model developed based on it with the help of Matlab-Simulink software is presented in Fig. 4b. A discrete signal defining the motion direction and the step pulses is delivered to input of control system of the stepping motor. It is assumed in the model of the setting assembly that only the n signal, corresponding to the number of the steps to be made by the rotor of the stepping motor, is conveyed to its input. The control system transforms it into the number of the impulses to be transmitted to the motor card, with adjusted frequency below the maximum operational frequency (here 1 kHz).

In order to model such an operation of the control system the signal steep limiter (frequency limiter) to 1000/per second has been used. The output of the element delivers a linearly growing or falling signal, marked as n', The block named *Dyskryminator* (*Discriminator*) transforms the linear signal into a stepped one, marked as n", with each step corresponding to one motor step. Since the motor control card enables operation in the following modes: 500, 1000,2000, and 4000 steps/per one revolution, the model is provided with an element named *Sterowanie uzwojeń (Winding control)*, enabling adjustment of one of the above mentioned divisions of a single step angle. Dynamics of the stepping motor (execution of one step after the moment of voltage application to the winding) is described by transmittance of the oscillating element. Based on the motor catalogue data and own research it was assumed that T_{sk}=0.0017s, ζ_{sk}=0.6. The last element of the assembly model is the screw of 0.5mm pitch. The output signal is the linear displacement x of the hydraulic amplifier slide.

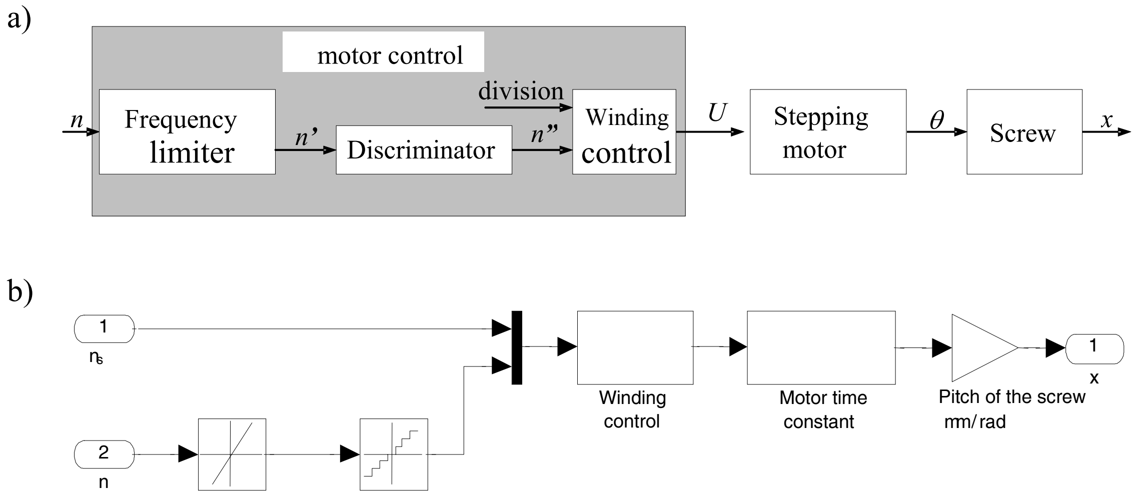

Figure 4: Model of the setting element with the stepping motor and the screw: a) block diagram; b) scheme of the simulation model.

3 The theoretical and simulation model of the four-edge amplifier

Figure 5 presents a four-edge hydraulic amplifier. Its input signals are pressure values p_0, p_T, and p_a and p_b, with output signals being Q_a and Q_b. In all the considerations a constant pressure p_0 has been assumed. Despite the fact that the outflow pressure p_T depends on resistance of the flow in the pipes between the valve and the container, for small flux intensity it may be assumed as equal to 0.

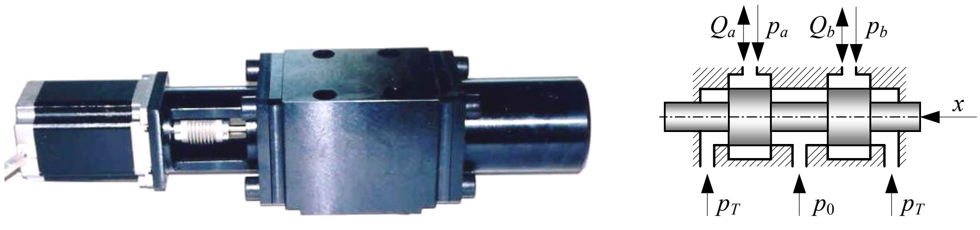

Figure 5: Four-edge amplifier.

The sleeve of the four-edge amplifier designed by the author includes four rhombus-shaped windows, of the angle 60º.

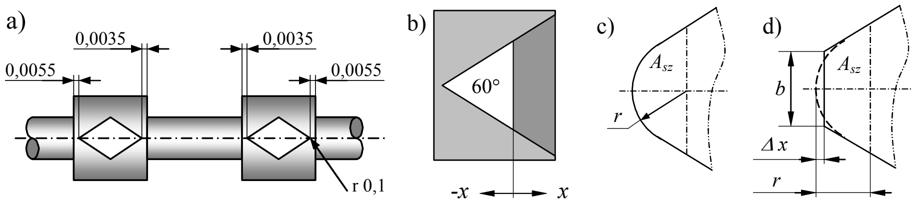

Figure 6: The hydraulic amplifier: a) results of overlap measurement;
b) slot; c) real corner shape; d) the corner shape assumed for the simulation model.

Figure 6a shows only two of them (the others are located at the other side of the slide). Figure 6a displays the distances between the window corners and the slide edge. Consideration of the corner rounding radius (equal to 0.1 for the considered amplifier) gives the slot area of the hydraulic amplifier (Fig. 6c) for the slide travel $\Delta x<1/2\cdot r$ that is determined by the formula:

$$A_{sz}=r^2\cdot\arccos\left(\frac{r-x}{r}\right)-\sqrt{2x\cdot r-x^2}\cdot(r-x) \qquad (1)$$

In case of larger displacements the area may be defined by the equation

$$A_{sz}=r^2\left(\frac{\pi}{3}-0{,}5\cdot\cos\frac{\pi}{6}\right)+(x-r)^2\cdot\tan\frac{\pi}{6}+2\cdot x\cdot(x-r)\cdot\cos\frac{\pi}{6} \qquad (2)$$

where: r – the radius of the slot corner.

Complex character of the formula practically prevents its application to the model (the simulation computation would be considerably longer) and, therefore, the real corner shape being a circular sector is approximated by a trapezoid (Fig. 3d). Areas for r displacement of the circular A_{szr} and trapezoidal A_{szm} slots are given by the following equations:

$$A_{szr}=\frac{\pi\cdot r^2}{3}+2\cdot r^2\cdot tg30° \qquad (3)$$

$$A_{szm}=\frac{4\dfrac{r}{\cos 30°}-2(r-\Delta x)\cdot tg30°}{2}\cdot(r-\Delta x) \qquad (4)$$

In order to keep good compliance of the approximation with reality, the b and Δx values were so defined as to give the area A_{szr} of the real slot approximately equal to the trapezoidal slot area A_{szm} for slide travel $x=r$. Some transformations provide:

$$\Delta x = r \cdot \left(1 - \sqrt{\frac{\pi}{12 - tg30°}}\right) \approx 0{,}3266 \cdot r \tag{5}$$

$$b = 2\left(\frac{r}{\cos 30°} - (r - \Delta x) \cdot tg30°\right) \approx 1{,}155 \cdot r \tag{6}$$

As was mentioned before, the slide may travel in both directions with regard to the zero position and, therefore, the *x* signal may take positive and negative values. As the slot area must not be negative, the formula includes absolute value of *x*. Substitution gives the following approximate formula for the slot area of the hydraulic amplifier:

$$A_{sz} = 2 \cdot \left(1{,}155 \cdot r \cdot |x| + 0{,}58 \cdot x^2\right) \tag{7}$$

In order to recognize better the phenomena occurring in the servo-unit, the preliminary experimental tests have been carried out, consisting in measuring the piston speed changes during opening of the slots of the so designed amplifier (slide motions in both directions with regard to the zero position). The results are shown in Figure 7.

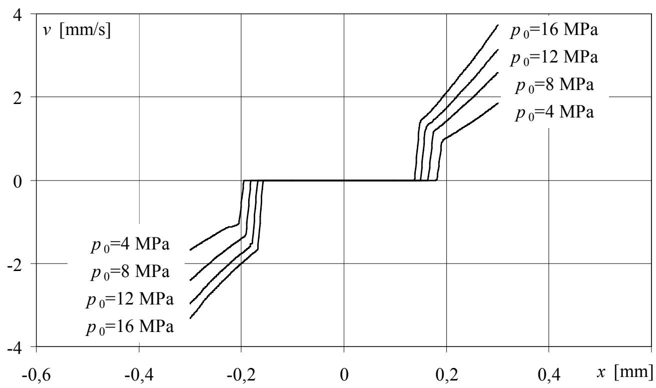

Figure 7: Speed change curves of the servo-unit piston during preliminary experimental tests for slow motion of the slide from neutral position.

The curves allow to state that after a certain standstill period the slide slots are choked in result of contamination. In order to start the piston the slide must be displaced even by 0.15mm. This results in nearly sudden speed growth from 1.0 to 1.5mm/s (according to the feed pressure). Such behaviour of the drive gives evidence of large number of contamination particles accumulated near the slide edges (the feeder was provided with the 10μm filter). According to author's opinion, the phenomenon may be caused by rotating and pressing the contamination particles located at the slide piston circumference into the slots. According to the above presented diagrams the slide travel required to unchoke the amplifier slots depends on the supply pressure of the servo-drive and the sense of the piston speed vector.

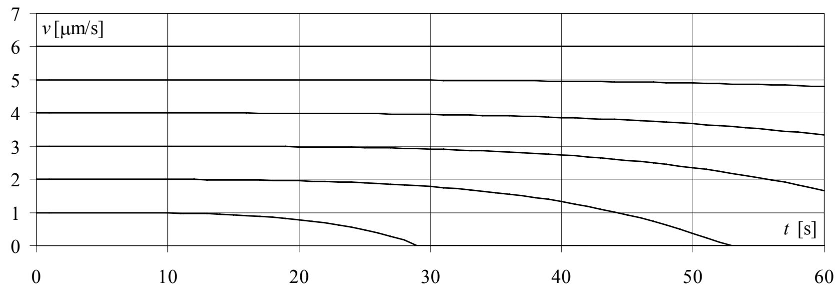

Figure 8: Speed change curves of the servo-unit piston for a small opening (choking of the working slots) registered during the experience tests.

Figure 8 shows the speed change curves of the piston of hydraulic servo-unit for a small opening of the hydraulic amplifier, registered during the experimental tests. It becomes clear that after expiration of a certain time, that depends on the valve opening, the piston speed drops until total stop. It means that operation with small velocity (i.e. for small opening) results in choking the valve slot.

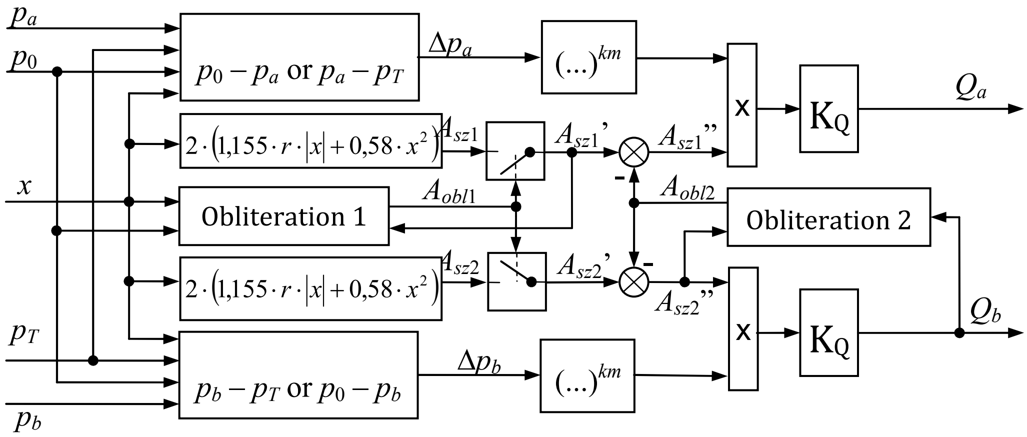

Figure 9: Block diagram of the model of four-edge hydraulic amplifier.

General block diagram of the four-edge hydraulic amplifier designed by the author is shown in Fig. 9. Signal values corresponding to pressure drops Δp_a and Δp_b at the choking slots are defined according to the slide travel sense. Afterwards, the pressure drop signals are raised to k_m power, equal to 0.538, that was experimentally determined. The slot areas A_{sz1} and A_{sz2} are calculated for the model with the use of the formula (7).

In order to model of the above investigated and described phenomenon of choking the slot during its opening the *Obliteration 1* block is used. Theoretical determination of the parameters that could characterize the phenomenon is in practice impossible, as it depends on such factors as the pressure in the slot, degree and type of the liquid contamination, duration of valve operation, liquid viscosity. The silting up is, to remarkable degree, of random character. Therefore, the parameters characterizing the phenomenon for various feed pressure values p_0 have been experimentally determined by preliminary tests of the valve (Fig. 7).

The block *Obliteration 2* models the process of silting up of the slot under its small opening, when it is choked in result of accumulation of tarry particles or other contamination, already after a short time [19]. Theoretical determination of such a process is very difficult too. Decrease of the liquid flux area depends chiefly on the slide travel, flux intensity, and duration of the flow of the value below the level corresponding to permanent flow capacity of the control device. Once the liquid compressibility may be neglected, the choking rate may be assumed to depend only on the flux value Q_a in a single chamber of the servo-motor. Figure 10 shows the diagram of the hydraulic amplifier model made with the help of Matlab Simulink. The model considers the phenomena characteristic for small fluxes. The switches 1 and 2 trigger the pressure signals, according to the sense of the slide motion, and in accordance with the principle: „ if $x \geq 0$ then : $\Delta p_a = p_0 - p_a$, $\Delta p_b = p_b - p_T$, otherwise: ($x < 0$) $\Delta p_a = p_a - p_T$, $\Delta p_b = p_0 - p_b$”. The blocks *Przekrycie 1* and *2* (*Overlap 1* and *2*) model overlapping of each of the amplifier slots. The formula (6) is encoded in the blocks A_{sz1} and A_{sz2}. In order to model the obliterations arising while opening the slots (*Obliteration 1*) the switches 3 and 4 are used They determine the choking ($A_{sz1}= A_{sz2}=0$) or unchoking condition. They are controlled by output signal of the function:

$$f(u) = |x| + p_0 \cdot k_{p0} + A_{sz1} \cdot k_{As} \tag{8}$$

where: k_{p0} , k_{As} – the coefficients found experimentally based on Fig. 7.

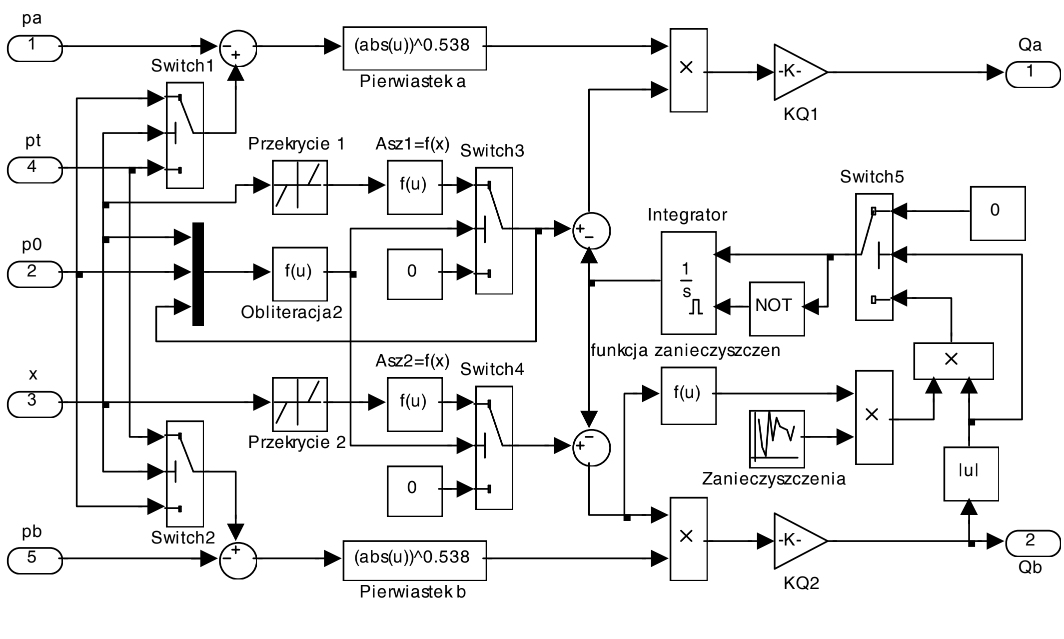

Figure 10: Simulation model of the four-edge amplifier.

The signal generated by it depends on slide travel, feed pressure, and the slot area. Assuming that the valve is initially closed ($x = 0$, $A_{sz1} = 0$), the input signal of the function *f(u)* depends only on the feed pressure. The switches are set to the state corresponding to choking of both slots. Gradual displacement of the slide (i.e. increase of x signal) results in growth of the output signal of the function and, once a certain experimentally determined threshold value is exceeded, the switches 3 and 4 are triggered. The signals corresponding to areas of the slots suddenly appear at their inputs. According to the formula (5.7) the signal depicting the A_{sz1} slot area is delivered to input of the *f(u)* function, thus increasing its output signal and resulting in positive feedback that models the valve hysteresis. Once the slot is unchoked, its next closing requires displacement of the slide to the position near to neutral $x \approx 0$ (the signal $A_{sz1} \cdot k_{As}$ increases value of the signal that controls the switches).

For modeling of choking of the slots that occurs at very slow flux the *Switch5* is used. When at its control input the absolute flux value exceeds a certain experimentally determined level corresponding to the piston velocity equal to 6μm/s, the output of the switch emits zero signal, meaning that the slots are not choked. For smaller opening the output of the switch 5 emits the signal equal to the product of two signals: the flux intensity and so-called “contamination”. The last one of them models the number of contamination particles flowing through the slot per unit of time. It is equal to the product of two other the signals: the random one and the one being inversely proportional to the slot area. In order to prevent division by 0 the last factor is modeled by the function $f_z(u) = 1/(A_{sz} + 0{,}00001)$. This allows for modeling the effect of the growth of choking of the slots at their small opening. The output signal from the switch 5 is delivered to an integrating element that sums the accumulating contamination versus time. This results in computation of the growth in time of the area A_{sz} taken by contamination in the slot of the amplifier. In the subtracting nodes of the model the areas of open working slots of the amplifier are reduced by the contaminated area. Should the flux intensity exceed a certain minimum value, the NOT element resets to zero the integrating member. This means that the whole contamination is torn away from the working slots and, in consequence, the block modeling the process of choking of the amplifier slots is switched off.

4 Theoretical model of the hydraulic servo-motor with unilateral piston rod

The hydraulic servo-motor are at present provided with seals of very good parameters. Therefore, it may be assumed that the flux intensity at the piston and piston rod are equal to zero. Hence, the components describing the leaking, that include coefficients KVab and KVb, may be neglected. This simplifying assumption transforms the system of equations of the hydraulic servo-motor to the form:

$$Q_a(t) = Q_{sa}(t) + Q_{ha}(t)\,, \quad Q_b(t) = Q_{sb}(t) + Q_{hb}(t) \tag{9}$$

$$A_a = A, \quad A_b = aA \ \ (a < 1) \tag{10}$$

$$Q_{ha}(t) = A\frac{dy(t)}{dt} \quad Q_{hb}(t) = aA\frac{dy(t)}{dt} \tag{11}$$

$$Q_{sa}(t) = \frac{V_a}{E_0}\frac{dp_a(t)}{dt} \quad Q_{sb}(t) = -\frac{V_b}{E_0}\frac{dp_b(t)}{dt} \tag{12}$$

$$m\frac{d^2y(t)}{dt^2} + f_{Td}\frac{dy(t)}{dt} = F_{obc} + A[p_a(t) - ap_b(t)] \tag{13}$$

where: Q_{ha}, Q_{hb} – absorbing capacity of the servo-motor chambers, Q_{sa}, Q_{sb} – the intensity that compensates the loss due to liquid compressibility, V_a, V_b – volumes of the working chambers in middle position of the piston, f_{Td} – coefficient of dynamic friction [N·s/m].

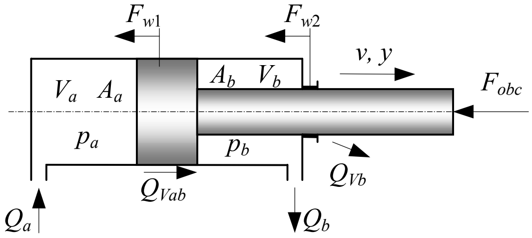

Figure 11: Servo-motor with unilateral piston rod.

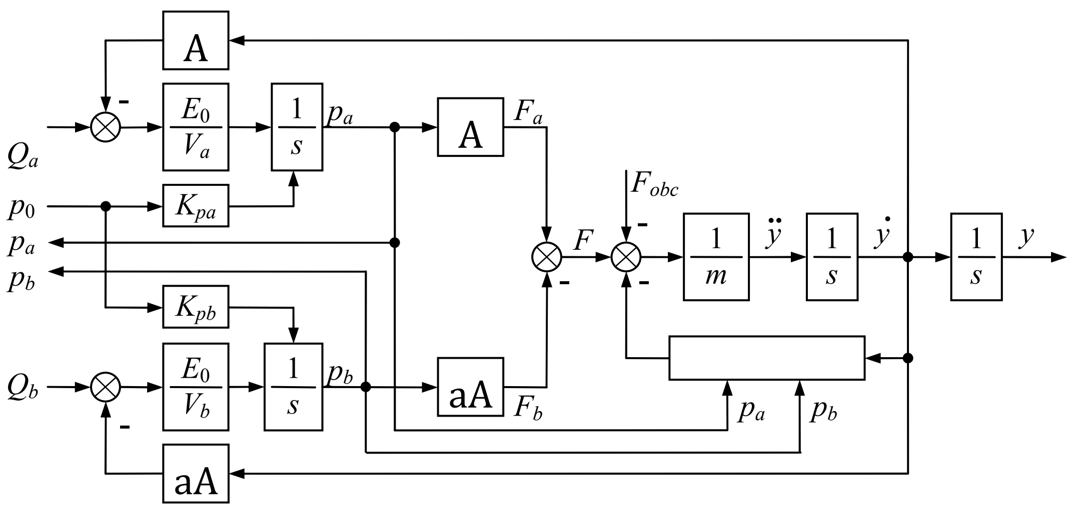

Figure 12: Block diagram of the model of a hydraulic servo-motor with unilateral piston rod.

The above system of equations served as a basis for developing the servo-motor block diagram, shown in Fig. 5.9. It includes an additional nonlinear block that models the resistance force F_U (inclusive of the friction at the seals), depending on the velocity and the pressures in the servo-motor chambers. The way of its modeling is presented in further part of the present chapter. The input signals of the servo-motor model are: flux intensity of the liquid flowing into the chambers and the force load F_{obc}. The output signals are: servo-motor piston position y and the pressures in servo-motor chambers p_a and p_b, that are transmitted to the model of the hydraulic amplifier (Fig. 10). Since the servo-motor is asymmetric, the flux intensities in the input and output windows of the hydraulic amplifier are not equal. Similarly, the pressures in the servo-motor chambers are different too. In consequence, the simulation model includes two patterns of signal courses, i.e. Q_a, p_a, F_a oraz Q_b, p_b, F_b.

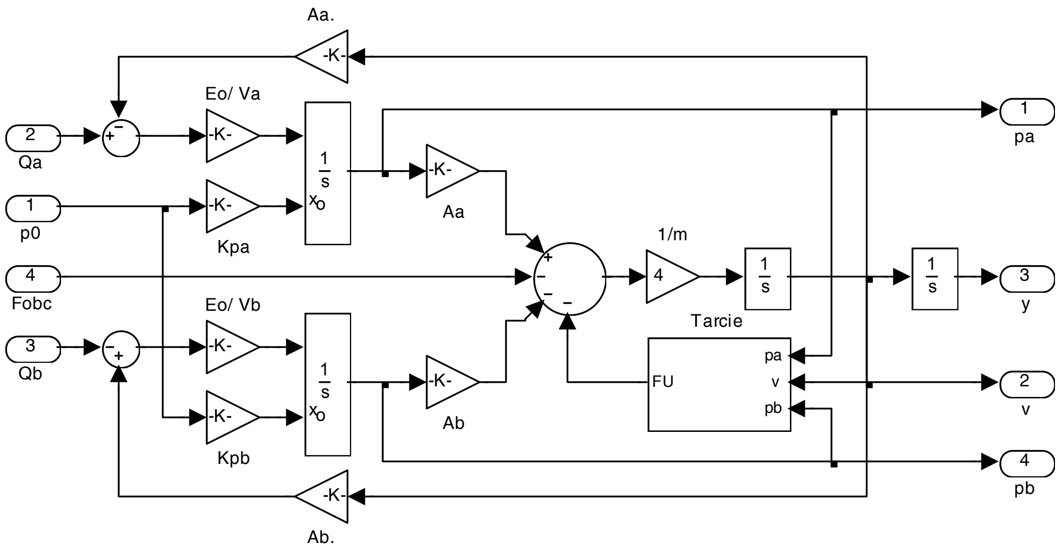

Figure 13: Simulation model of a hydraulic servo-motor with unilateral piston rod.

Figure 13 shows the model of the hydraulic servo-motor developed by the author in the Matlab-Simulink software. Initial values of p_a and p_b pressures are set to the values formerly determined experimentally, according to the pressures occurring in servo-motor chambers in steady state, i.e. after cutting off the feed to and outflow from the chambers (provided that the servo-motor was fed and moved). According to the tests, in case of good tightness of the amplifier and servo-motor such a condition lasts more than ten minutes after displacing the slide to neutral position. The following values of the coefficients are adopted:

- servo-motor of piston diameter 100mm, piston rod diameter 60mm and travel 400mm;
- piston area A_a = 7854 mm^2, and A_b = 5027 mm^2 (a = 0,64),
- $1/m$ = 4 mm/(N·s^2), (1/kg = m/(N·s^2) = 1000 mm/(N·s^2)
- coefficient of initial pressure: K_{pa} = 0,471 and K_{pb} = 0,735, respectively;

− stiffness of the left-hand and right-hand servo-motor chambers: E_0/V_a = 7,64 · 10^{-4} N/mm^5 and E_0/V_b = 11,94 · 10^{-4} N/mm^5 (E_0 = 1,2 · 10^3 MPa), respectively.

5 Simulation tests of electro-hydraulic servo-drive with electric feedback

Figure 14 presents the block diagram of the simulation model of electro hydraulic servo-drive with stepping motor, electric feedback, and controller. The patterns obtained from the simulation and presented in Fig. 15 show possible applications of the procedure of setting the neutral position of the slide. The simulation tests indicated usefulness of the procedure in setting the initial position of the valve and further correct operation of the controller assembly.

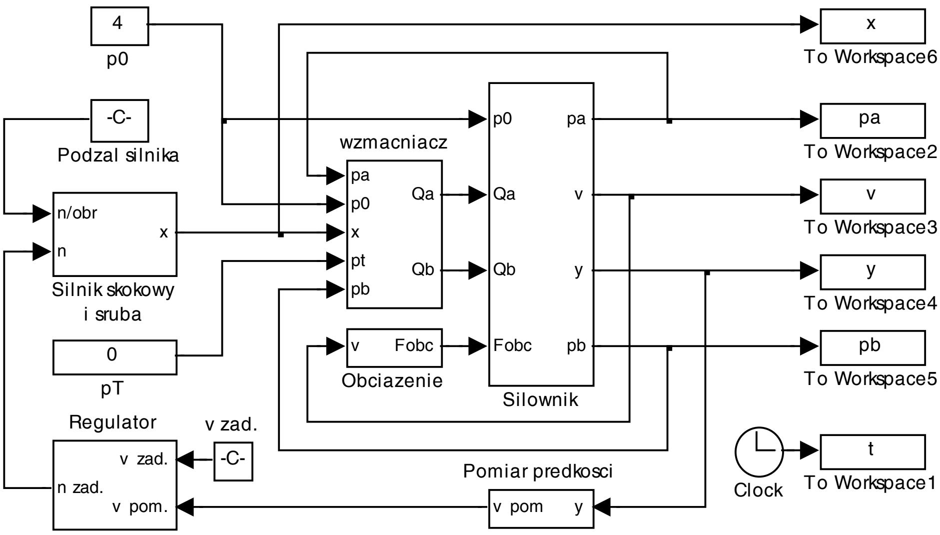

Figure 14: Block diagram of the complete simulation model of electro-hydraulic servo-unit provided with stepping motor and feedback.

Fig. 15 shows the time-curves obtained in the course of the simulation, while displacing the slide of the hydraulic amplifier along the triangle curve, with the rate of 100 steps/per second. The time-velocity curve recorded in the simulation shows the process of obliteration of the slots, moreover, and reflects the square relationship between the slide displacement and flux intensity. Piston motion was initiated only after about 200 steps of the motor.

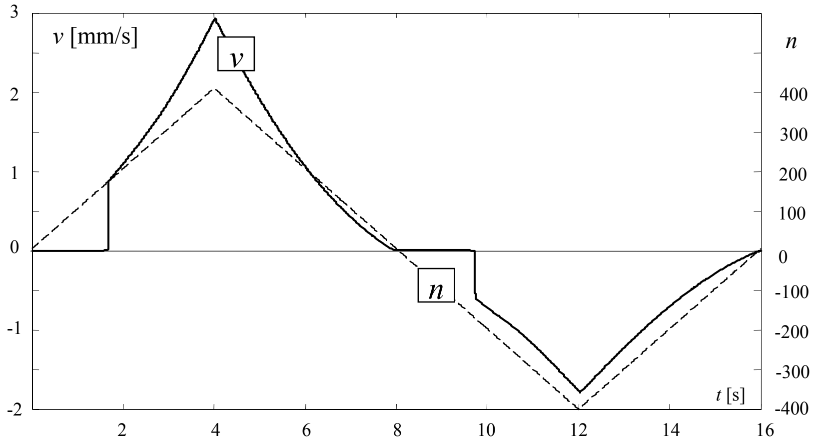

Figure 15: Time pattern of the valve characteristics, with setting signal (for feeding pressure 4MPa.

6 Experimental tests of the servo-unit

According to initial experimental tests of the model (Figs 7, 8) and simulation tests of the hysteresis (Fig. 15) the operational characteristics of the servo-unit for slide displacements in the range 0-0.2mm (choking of the slots) undergoes very large changes. Therefore, experimental verification of the simulation results becomes important and, an algorithm for experimental recording of the hysteresis has been developed. In order to compare the simulation and experimental tests the same conditions of the servo-unit operation have been adopted in both tests. Results of the tests are shown in Fig. 16, where the time pattern of the slide position and piston velocity for feeding pressure equal to 4MPa are presented. The relationship between velocity and travel of the slide of hydraulic amplifier is presented too. Comparison of the experimental and simulation tests of the hysteresis (Fig. 15) shows high similarity of the patterns. This gives evidence of correctness of theoretical model of the servo-unit and the simulation model developed based on it.

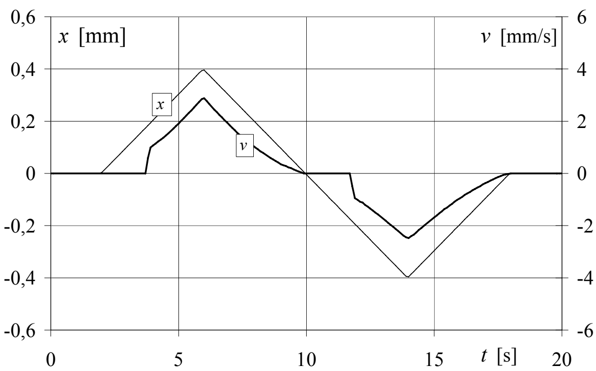

Figure 16: Time pattern of the process of investigation of hysteresis of the hydraulic amplifier (for feeding pressure of 4MPa).

The tests of the servo-unit indicated that the use of proper control program that enables opening and closing the valve with high frequency, allows to initiate its motion with velocity of the order of several μm/s. An incremental straight-edge assembled at the stand gave the resolution of 0.5μm and, therefore, the measurements were charged with large errors. Low and very low motion velocities are measured with an indirect method. The measurement error (Δv) depends on the error of displacement variation error and time measurement error. Very low velocities of the electro hydraulic servo-unit have been measured with the ML 10 laser measuring interferometer from Renishaw (Fig. 17) of the accuracy 0.05μm and resolution 0.01μm.

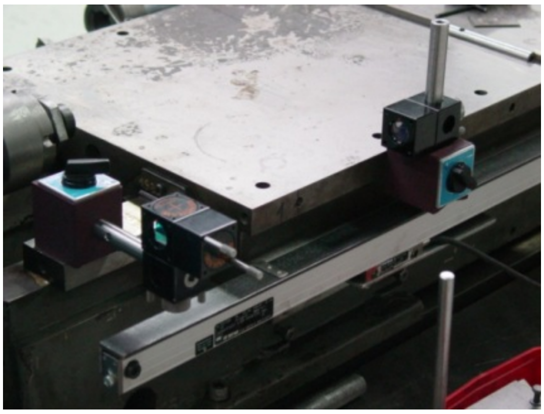

Figure 17: Measurement of displacement changes and velocity of the tested servo-unit with the Renishaw ML 10 interferometer.

The limiting error of velocity measurement for this method amounted to 1μm. Figure 18 presents the results of the patterns of displacement changes and velocity recorded during experimental tests of the servo-unit with the use of the interferometer.

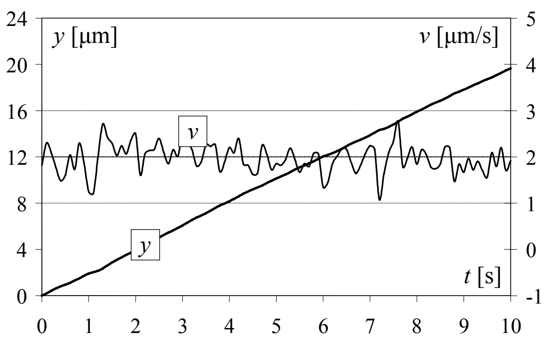

Figure 18: The patterns of displacement changes and velocity recorded with the Renishaw system for the velocity v=2μm/s.

Presentation of the results charged with so large relative error of the measurement remains justified, as they allow to check whether the motion is or is not accompanied by piston rod vibration (the "stick-slip" effect). The vibration would be visible on the recorded curves. The plot shown in Fig. 18 allows to state that the vibration does not occur or its amplitude does not exceed 0.1μm. During measurement the data have been so adjusted as to determine the velocity in time ranges of 1s. This allowed to reduce the measurement error to 0.1μm/s.

The above enables to state that the electro-hydraulic servo-unit provided with stepping motor and electric feedback moved with uniform velocity (that was difficult to determined because of measurement reasons).

7 Summary

Based on theoretical considerations and the simulation and experimental tests of the electro-hydraulic servo-unit, with stepping motor, acting as a setting element, and electric feedback it is concluded that the use of the stepping motor for setting the travel of the slide of the hydraulic amplifier is possible and it enables very small and accurate slide displacements to be achieved.

Such a solution ensures that the flux control valve can be set with high precision and enables very slow motion of a servo-unit provided with such a valve. The minimum feasible permanent speed of the servo-unit considered amounted about to 2μm/s. Reduction of the minimum speed is limited by the low frequency of the digital measurement of low velocity and contamination of the liquid resulting in obliteration of small slots. The possibility of achieving a low velocity for the rotational motion of the slide is controlled by removal of the contamination accumulating at the edges of the working slots. Contamination particles of the dimensions exceeding the slot area may flow as a result of the temporary increase in the slot area as a result of slide oscillation. The amplitude and frequency of the oscillation is particularly important. Servo-units provided with electric feedback may ensure the high flexibility of the adjustment of the parameters and compensation of the nonlinearity. Nevertheless, this required the use of a more sophisticated control system. The slide valve with triangular slots used here for controlling small liquid fluxes requires the use of a special forcing procedure during its opening. This leads to the need of improving the control algorithm. Optimization of the parameters of various types of controllers and control algorithms and verification of usefulness and purposefulness of their use for controlling the servo-unit provided with electric feedback enables achieving low and very low speeds of motion.

References

[1] Becker M., "Schrittmotor als aktuator fur hydraulik-wegeventile", Öilhydraulik und Pneumatic, Volume 4, 2000.

[2] Faulhaber S., “Stationarily accurate postion controls at an example of a hydraulic servodrive”, Öilhydraulik und Pneumatic, Volume 30, Issue 6, 453-456, 1986.
[3] Freitag E., “Polyurethannutinge mit verringerter reibung”, Öilhydraulik und Pneumatic., Volume 2, 2001.
[4] Staniek R., “Researches of electrohydraulic drive with a mechanical feedback linkage”, Structural Dynamics and Vibrations, PD-Vol. 63, 43-46, 1994.
[5] Staniek R., “The influence of hydraulic feedback upon the stability of linear drive in extrusion presses”, Structural Dynamics and Vibrations, PD-Vol. 70, 5-10, 1995.
[6] Ulacia I., Salisbury C.P., Hurtado I., Worswick, M.J. “Tensile characterization and constitutive modeling of AZ31B magnesium alloy sheet over wide range of strain rates and temperatures”, Journal of Materials Processing Technology, Vol. 211, Issue 5, 830-839, 2011.
[7] http://www.victorycontrols.com/ (15.04.2012)
[8] http://www.eaton.com/ (15.04.2012)
[9] http://www.boschrexroth.com/ (15.04.2012)
[10] http://www.hydraulichouse.com/ (15.04.2012)
[11] http://www.moog.com.sg/ (15.04.2012)